SCHOOL OF MATERIALS AND MINERAL RESOURCES ENGINEERING
UNIVERSITI SAINS MALAYSIA

SYNTHESIS OF METAL OXIDE COUPLED TiO_2 PHOTOCATALYST PARTICLES FOR ENHANCED PHOTODEGRADATION OF RHODAMINE B DYE

By

TAN ZHUANG MIN

Supervisor: Dr. Sivakumar A/L Ramakrishnan

Co-Supervisor: Assoc. Prof. Ir. Dr. Pung Swee Yong

Dissertation submitted in partial fulfillment
of the requirements for the degree of Bachelor of Engineering with Honours
(Materials Engineering)

UNIVERSITI SAINS MALAYSIA

15 JULY 2022

DECLARACTION

I hereby declare that I have conducted, completed the research work and written the dissertation entitled "**Synthesis of Metal Oxide Coupled TiO_2 Photocatalyst Particles for Enhanced Photodegradation of Rhodamine B Dye**". I also declare that it has not been previously submitted for the award of any degree or diploma or other similar title of this for any other examining body or university.

Name of student: Tan Zhuang Min Signature:

Date: : 15 July 2022

Witnessed by

Supervisor: Dr. Sivakumar A/L Ramakrishnan Signature:

Date : 15 July 2022

Co-Supervisor: Assoc. Prof.Ts.Ir. Dr. Pung Swee Yong Signature:

Date : 15 July 2022

ACKNOWLEDGEMENT

First of all, I would like to express my deepest gratitude towards University Sains Malaysia and School of Materials and Mineral Resources Engineering for providing all equipment and facilities required for the practical work of this project. I would like to thank my supervisor Dr. Sivakumar A/L Ramakrishnan and my co-cupervisor Assoc. Prof.Ts.Ir. Dr. Pung Swee Yong for guiding me through this project with patience. I would also like to thank Prof. Ir. Dr. Mariatti binti Jaafar Mustapha for generously providing grant (grant number: 308 AIBAHAN 415403) to make this project possible.

Besides, my sincere appreciation to the technical staffs of School of Materials and Mineral Resources Engineering, Puan Haslina binti Zulkifli, Encik Mohammad Azrul bin Zainol Abidin, and Encik Mohamad Syafiq bin Mustapa Sukri for providing their technical knowledge and support during my research works. Without the assistance of the technical staffs, this project would have been considerably more difficult to accomplish

Lastly, I must thank my beloved friends, seniors and family for their continuous support and motivation throughout this challenging journey. They have shown me so much encouragement so that I can pursuit my research with persistence.

TABLE OF CONTENTS

DECLARACTION ..... **I**

ACKNOWLEDGEMENT ..... **II**

TABLE OF CONTENTS ..... **III**

LIST OF TABLES ..... **VI**

LIST OF FIGURES ..... **VII**

LIST OF ABBREVATIONS ..... **X**

LIST OF SYMBOLS ..... **XI**

INTRODUCTION **1**

1.1 Background 1

1.2 Problem Statement 3

1.3 Research Objectives 3

1.4 Scopes of Research 4

1.5 Dissertation Outline 4

CHAPTER 2 LITERATURE REVIEW **5**

2.1 Photocatalysis 5

2.2 Titanium(IV) Oxide (TiO_2) 7

2.2.1 Limitation of TiO_2 11

2.3 Semiconductor Heterojunction 12

2.3.1 Z-Scheme Photocatalytic Systems 15

2.3.2 Direct Z-Scheme Photocatalysts 16

2.4 Modification of TiO_2 through Coupling 18

2.4.1 CuO/TiO_2 Photocatalyst Composite 19

2.4.2 ZnO/TiO_2 Photocatalyst Composite 19

2.4.3 SnO_2/TiO_2 Photocatalyst Composite 21

2.5 Structure and Morphologies of Photocatalysts 22
2.6 Photodepositon.....26
2.7 Thermal Oxidation of Metal.....32
2.7.1 Thermal Oxidation of Tin 33
2.7.2 Thermal Oxidation of Copper..... 34
CHAPTER 3 RAW MATERIALS AND METHODOLOGY 36
3.1 Introduction.....36
3.2 Raw Materials 38
3.3 Experimental Procedure.....38
3.4 Characterization Techniques.....41
3.4.1 FESEM..... 41
3.4.2 EDX 42
3.4.3 XRD 42
3.4.4 UV-Vis Absorption Spectroscopy 43
CHAPTER 4 RESULTS AND DISCUSSIONS 45
4.1 FESEM and EDX Analysis.....45
4.2 XRD Analysis 54
4.3 Photocatalytic Performances of Metal Oxide Coupled TiO_2 Particles 58
4.3.1 Photocatalytic Performance of Uncoupled TiO_2 Particles..... 58
4.3.2 Photocatalytic Performance of CuO/TiO_2 Particles..... 60
4.3.3 Photocatalytic Performance of ZnO/TiO_2 Particles..... 62
4.3.4 Photocatalytic Performance of SnO_2/TiO_2 Particles..... 65
CHAPTER 5 CONLUSION AND RECOMMENDATIONS 71
5.1 Conclusion 71
5.2 Recommendation for future work.....72

Reference 73

APPENDIX A 80

APPENDIX B 81

APPENDIX C 83

APPENDIX D 87

APPENDIX E 88

APPENDIX F 89

APPENDIX G 90

Appendix H 91

Appendix I 92

LIST OF TABLES

Table 2.1: Crystal properties of rutile, brookite and anatase (Oi et al., 2016) 9

Table 2.2: Summary of works done by researchers on synthesis of coupled photocatalysts by photodeposition method 31

Table 3.1: List of raw materials used for this project 38

Table 3.2: Amount of precursor used to prepare 2 mM metal solution 39

Table 3.3: Denotation of Samples 40

Table 4.1: Average particle sizes of uncoupled TiO_2 and various metal oxide coupled TiO_2 particles 50

Table 4.2: Element compositions of CuO coupled TiO_2 particles 51

Table 4.3: Element compositions of ZnO coupled TiO_2 particles 52

Table 4.4: Element compositions of SnO_2 coupled TiO_2 particles 53

LIST OF FIGURES

Figure 2.1: Different possibilities of reactions. (A) Reduction. (B) Oxidation. (C) Redox reaction. (D) No reaction (Ameta et al., 2018)..... 6

Figure 2.2 Crystal structures of rutile, brookite and anatase (left to right) (Moellmann et al., 2012) 9

Figure 2.3: Initial rate for the decomposition of four different pollutants in aqueous solution using different TiO_2 commercial photocatalysts with anatase structure (A, Millenium), rutile (R), or a mixture of rutile and anatase (A+R, Evonik-Degussa P25) (Hernández-Alonso et al., 2009)..... 10

Figure 2.4: Types of heterojunction system of coupled semiconductors (Janczarek & Kowalska, 2017) 13

Figure 2.5: The charge transfer in a type II heterostructure (Xu et al., 2018) 14

Figure 2.6: The charge transfer in a direct Z-scheme heterostructure (Xu et al., 2018) 15

Figure 2.7: Semiconductor-semiconductor junction with staggered band configurations (a) in contact without photon irradiation (b) in contact with photon irradiation..... 17

Figure 2.8: p-n junction (a) in contact without photon irradiation (b) in contact with photon irradiation..... 18

Figure 2.9: Schematic diagram of the charge-transfer process in the TiO_2/SnO_2 nanotubes composite photocatalysts (Hou et al., 2007)..... 22

Figure 2.10: Different core–shell nanostructures: (a) core is a single sphere, (b) core with multiple concentric shells, (c) shell incorporated with smaller spheres, (d) shell in the form of identical smaller spheres, and (e) shell in the form of different spheres, (f) solid core and porous shell, (g) core–shell both porous, (h) multiple spherical cores, (i) multiple cores covered by shell formed by several small spheres, (j) core–shell fiber,

and (k) yolk–shell morphology shows a movable core within a hollow shell. (Mondal & Sharma, 2016)..... 24

Figure 2.11: The morphologies of RuO_x on TiO_2 films produced by photodeposition without methanol (left) and with methanol (right) 27

Figure 2.12: Schematic illustration of construction of $CdS@MoO_x$ 29

Figure 3.1: Overall flow chart of this project 37

Figure 3.2: Temperature profile of annealing process 40

Figure 4.1: FESEM image of TiO_2 particles (a) before and (b) after annealing at 600 °C in ambient atmosphere for 2 h under 30kX magnification 46

Figure 4.2: FESEM image of (a) CuO/TiO_2 (25,1), (b) CuO/TiO_2 (50,1), (c) CuO/TiO_2 (25,3) and (d) CuO/TiO_2 (50,3) under 30kX magnification 47

Figure 4.3: FESEM image of (a) ZnO/TiO_2 (25,1), (b) ZnO/TiO_2 (50,1), (c) ZnO/TiO_2 (25,3) and (d) ZnO/TiO_2 (50,3) under 30kX magnification 48

Figure 4.4: FESEM image of (a) SnO_2/TiO_2 (25,1), (b) SnO_2/TiO_2 (50,1), (c) SnO_2/TiO_2 (25,3) and (d) SnO_2/TiO_2 (50,3) under 30kX magnification 49

Figure 4.5: XRD result for TiO_2 particles before and after annealing at 600 ºC for 2 h in ambient atmosphere 55

Figure 4.6: XRD result for CuO coupled TiO_2 particles ..... **Error! Bookmark not defined.**

Figure 4.7: XRD result for ZnO coupled TiO_2 particles..... **Error! Bookmark not defined.**

Figure 4.8: UV-Vis spectra of RhB solution photodegraded by uncoupled TiO_2 particles ..... **Error! Bookmark not defined.**

Figure 4.9: (a) Photodegradation efficiency by uncoupled TiO_2 particles (b) Kinetic plot of photodegradation by uncoupled TiO_2 particles.....**Error! Bookmark not defined.**

Figure 4.10: Photodegradation efficiencies of uncoupled TiO_2 and various CuO coupled TiO_2 particles.....61

Figure 4.11: Photodegradation rate constants of RhB solution by various CuO/TiO_2 particles synthesized using different (a) methanol concentration and (b) deposition duration.....62

Figure 4.12: Photodegradation efficiencies of uncoupled TiO_2 and various ZnO coupled TiO_2 particles.....64

Figure 4.13: Photodegradation rate constants of RhB solution by various ZnO/TiO_2 particles synthesized using different (a) methanol concentration and (b) deposition duration.....65

Figure 4.14: Photodegradation efficiencies of uncoupled TiO_2 and various SnO_2 coupled TiO_2 particles.....66

Figure 4.15: Photodegradation rate constants of RhB solution by various SnO_2/TiO_2 particles synthesized using different (a) methanol concentration and (b) deposition duration.....67

LIST OF ABBREVATIONS

TiO_2	Titanium Dioxide
CuO	Copper(II) Oxide
ZnO	Zinc Oixde
SnO_2	Tin(IV) Oxide
RhB	Rhodamine B
CB	Conduction Band
VB	Valence Band
EDX	Energy-Dispersive X-ray
XRD	X-Ray Diffraction
FESEM	Field Emission Scanning Electron Microscopy
e^-	Electron
h^+	Holes
UV	Ultraviolet Light

LIST OF SYMBOLS

a.u.	Arbitraty unit
at%	Atomic percent
vol%	Volume percent
°	Degree
°C	Degree Celcius
min	Minutes
h	Hour
eV	Electron volt
%	Percent
k	Rate costant

SYNTHESIS OF METAL OXIDE COUPLED TIO_2 PHOTOCATALYST PARTICLES FOR ENHANCED PHOTODEGRADATION OF RHODAMINE B DYE

ABSTRACT

Environmental pollution is a global problem and dye pollution is one of the major factor. TiO_2 shows some promising photocatalytic properties that can degrade organic pollutant under UV irradiation. However, TiO_2 possesses some disadvantages such as wide band gap and high recombination rate of electron hole pairs. Coupling TiO_2 with various metal oxides can enhance the photocatalytic properties. This project has used photodepositon (reduction of metal ions on TiO_2) followed by thermal oxidation method for the coupling of TiO_2 with CuO, ZnO and SnO_2 under various methanol concentrations (25 vol% or 50 vol%) and deposition duration (1 h or 3 h) to observe the effect of these parameters on the photocatalytic degradation activity on rhodamine B dye (up to 90 mins). The rate constant of photodegradation reaction (k) has improved from 0.0141 min^{-1} (uncoupled TiO_2) to 0.0151~0.0368 min^{-1}. Overall, CuO/TiO_2 and SnO_2/TiO_2 samples have shown similar photocatalytic properties (average rate constants of 0.0341 min^{-1} and 0.0327 min^{-1} respectively), and both performed better than ZnO/TiO_2 in terms of RhB photodegradation (average rate constants of 0.0197 min^{-1}). The difference in photocatalytic performance can be explained by the bandgap of metal oxides and their relative band positions with TiO_2. Lastly, among CuO/TiO_2 and SnO_2/TiO_2 samples, CuO/TiO_2 (50,3) and SnO_2/TiO_2 (50,3) have shown the best photocatalytic properties respectively due to the longer deposition time and higher concentration methanol, resulting in more deposited materials.

SINTESIS OKSIDA LOGAM BERGABUNG ZARAH PEMANGKIN FOTO TIO_2 UNTUK PENINGKATAN FOTODEGRADASI RHODAMINE B DYE

ABSTRAK

Pencemaran alam sekitar adalah masalah global dan pencemaran pewarna adalah salah satu faktor utama. TiO_2 menunjukkan sifat fotokatalitik yang boleh merosakkan bahan pencemar organik di bawah penyinaran UV. Walau bagaimanapun, TiO_2 mempunyai beberapa kelemahan seperti bandgap yang lebar dan kadar penggabungan semula pasangan lubang-elektron yang tinggi. Gandingan TiO_2 dengan pelbagai oksida logam boleh meningkatkan sifat fotomangkin. Projek ini telah menggunakan pemendapan foto diikuti kaedah pengoksidaan terma untuk menggandingkan TiO_2 dengan CuO, ZnO dan SnO_2 di bawah pelbagai kepekatan metanol (25 vol% atau 50 vol%) dan tempoh pemendapan (1 jam atau 3 jam) untuk memerhatikan kesan parameter tersebut terhadap aktiviti degradasi fotomangkin pada pewarna rhodamine B (sampai 90 min). Pekali kadar tindak balas fotodegardasi (k) telah menaik daripada 0.0141 min^{-1} (TiO_2 sebelum penggabungan) kepada 0.0151~0.0368 min^{-1}. Secara keseluruhannya, sampel CuO/TiO_2 dan SnO_2/TiO_2 telah menunjukkan sifat fotokatalitik yang sama (pemalar kadar purata masing-masing 0.0341 min^{-1} dan 0.0327 min^{-1}), dan kedua-duanya lebih baik daripada ZnO/TiO_2 dari segi fotodegradasi RhB (pemalar kadar purata = 0.0197 min-1). Perbezaan dalam sifat fotokatalitik boleh dijelaskan oleh bandgap oksida logam dan kedudukan band berbanding dengan TiO_2. Akhir sekali, antara sampel CuO/TiO_2 dan SnO_2/TiO_2, CuO/TiO_2 (50,3) dan SnO_2/TiO_2 (50,3) masing-masing telah menunjukkan sifat fotomangkin terbaik disebabkan oleh masa pemendapan yang lebih lama dan metanol kepekatan yang lebih tinggi, menghasilkan lebih banyak bahan pemendapa

CHAPTER 1
INTRODUCTION

In this project, TiO_2 particles coupled with metal oxides will be synthesized by photodeposition of metal followed by thermal oxidation of the metal via annealing. Two synthesis parameters (concentration of methanol and deposition duration) will be varied to observe the effect of these parameters on the photocatalytic properties of the coupled TiO_2 particles as well as the morphology of the deposited metal oxide. Rhodamine B (RhB) dye solution will be photodegradated by the coupled TiO_2 particles for photocatalytic study. This chapter includes background, problem statement, research objectives, scope of research and dissertation outline.

1.1 Background

Environmental pollution is becoming an urgently global problem with the rapid development of industry. The textile industry, which involves the use of dyes that are difficult to degrade, is one of the major contributors to environmental pollution. Syuhadah (2017) has made a thorough review on water pollution by textile industry. More than 10,000 types of dyes are being used in the textile industries. During the production of textile, the remaining dyes that are not being incorporated into the fabric will become waste, and if the waste is not being treated prior to discharge, it can pollute the environment. Although most of the colours can stay on the fabrics, 30 to 40 percent of the dyes will be washed out directly into the environment or into the drainage system. The difficulty of treating dye containing effluents may become greater after they have entered the environment because the dyes have synthetic origin and complex molecular structure, which makes them more

stable and less biodegradable in that case. On top of that, the wastewater can be absorbed by terrestrial and aquatic plants, and the harmful chemical can be passed to animals in the food chain and even to humans. The toxic effects of dyes range from cancer and allergies to humans, to growth inhibitions of microscopic organisms and plants. Not only that, extensive water pollution from dyes can also cause damage to the country economy due to the generally expensive pollution clean-up procedure (Syuhadah, 2017).

Until today, several traditional approaches have been adopted to address organic pollution worldwide: membrane separation, flocculation-condensation, adsorption, oxidation or ozonation, reverse osmosis and many more. However, these approaches are unable to remove organic pollutants completely or effectively (Bai et al., 2021). Photocatalytic degradation of wastewater is a promising way owing to efficiency, green, environmental compatibility and convenience. Photocatalytic reaction is a heterogeneous reaction that occurs on the catalyst surface to accelerate the conversion of light energy into chemical energy, including excitation, redox reaction and recombination, and to achieve the potential balance between the Fermi energy level of the catalyst and the surface adsorbents (Bai et al., 2021). Metal oxide semiconductors are commonly used as photocatalysts for such application due to their electronic structure, light absorption properties and charge transport characteristics (Ameta et al., 2018). For enhanced photocatalytic properties, semiconductor heterojunction can be formed through the coupling of different metal oxide semiconductors. Besides, the metal oxides may exist in various morphologies, and the morphologies of each component was found to have influence on the overall photocatalytic properties of the semiconductor composite (will be further discussed in Section 2.5). In this project, TiO_2 will be used as the main photocatalyst for the photodegradation of dye. By coupling TiO_2 with other metal oxides (CuO, ZnO and

SnO_2 in this project), the photocatalytic properties of TiO_2 can be improved, providing a more efficient photodegradation of pollutant.

1.2 Problem Statement

1) Poor photocatalytic performance by TiO_2 particles for dye degradation

Despite all its attractive properties, the photocatalytic performance of pure TiO_2 is poor due to its large bandgap and fast recombination of charge carriers, making it less reliable for practical usage when it comes to photodegradation of dye and other organic pollutant.

2) Lack of understanding on the morphology of coupled metal oxides on the photocatalytic performance of TiO_2

Coupling of TiO_2 with metal oxide is one of the options to improve its photocatalytic performance. However, despite much research have been done on this subject, the coupled metal oxides in those research mainly exist as particulates on the surface of TiO_2. Besides, the use of TiO_2 as the core of a core-shell composite has never been studied; instead, research until today only explore the use of TiO_2 as the shell. The effect of having different morphologies of metal oxide on TiO_2 core on the combined photocatalytic performance remains unclear.

1.3 Research Objectives

1) Synthesize and characterize different metal oxide coupled TiO_2 photocatalysts for improved photodegradation of dyes with photodeposition method followed by thermal oxidation and see the effect of various bandgap of coupled metal oxide on the overall properties.

2) Control the morphologies of coupled metal oxides and observe the effect of various morphologies on the photocatalytic properties

1.4 Scopes of Research

In this project, TiO_2 particles coupled with metal oxides were synthesized using photodeposition followed by thermal oxidation. Two synthesis parameters were manipulated, which were the concentration methanol and the duration of photodepositon. The metal oxides to be coupled on TiO_2 were CuO, ZnO and SnO_2. The photocatalytic performance of the coupled TiO_2 particles on Rhodamine B (RhB) dye solution was characterized by using UV-Vis absorbance spectroscopy. Various characterization methods were carried out like Field-Emission Scanning Electron Microscope (FESEM) for surface morphology, Energy-Dispersive X-ray spectroscopy (EDX) for elemental composition and X-Ray Diffraction (XRD) for phase analysis.

1.5 Dissertation Outline

This thesis contains five chapters in total. Chapter One states the background, problem statement, research objectives and its scopes. Chapter Two mainly reviews some literatures regarding photocatalysis, TiO_2, semiconductor heterojunction, metal oxide coupled TiO_2, morphologies of composites, photodeposition method and thermal oxidation of metals.. Chapter Three describes experimental procedures and characterization techniques that were used in this research. Moreover, Chapter Four focuses primary on the analysis and discussion of the results obtained from this research. Lastly, Chapter Five outlines the conclusion for this research and recommendation for future work.

CHAPTER 2

LITERATURE REVIEW

2.1 Photocatalysis

A photocatalyst is a material that can convert light energy into chemical energy by absorbing light, bringing itself to a higher energy level to provide energy to a reacting substance and make a chemical reaction occur or change the rate of a chemical reaction (Oshida, 2013; Ameta et al., 2018). Generally, photocatalysts are semiconductor materials. Photocatalytic reaction or photocatalysis has great potential in many technologies such as water splitting to produce hydrogen and/or oxygen gas, reduction of carbon dioxide to produce hydrocarbon fuels, bacteria disinfection, selective synthesis of organic compounds and many more.

This project focuses mainly on using metal oxide coupled TiO_2 particles as photocatalyst for photodegradation of organic dye, hence understanding the basic mechanisms of photocatalytic reaction is crucial for explaining the behavior of these photocatalyst under the irradiation of light. In general, photocatalytic reaction can be broken down into 4 steps: (1) photon irradiation on the photocatalyst to induce photogeneration of electron-hole pairs, (2) charge carrier separation and migration to the surface of the photocatalyst, (3) reduction/oxidation reaction by the charge carriers, and (4) recombination of charge carriers in the bulk or on the surface of photocatalyst. These four steps are complementary, and the thermodynamics and kinetics of these processes determine the efficiency of a given photocatalyst (Xu et al., 2018). In step 3, the generated electron is used for reducing an acceptor whereas the generated hole is used for oxidation of donor molecules, hence a photocatalyst provides both oxidation and reduction

environment simultaneously (Ameta et al., 2018). The fate of photogenerated electrons and holes are decided by the relative positions of conduction band (CB) and valence band (VB) of the semiconductor and the redox levels of substrate; and the four possible relative positions of energy band and redox levels are summarized in Figure 2.1 by Ameta et al. (2018).

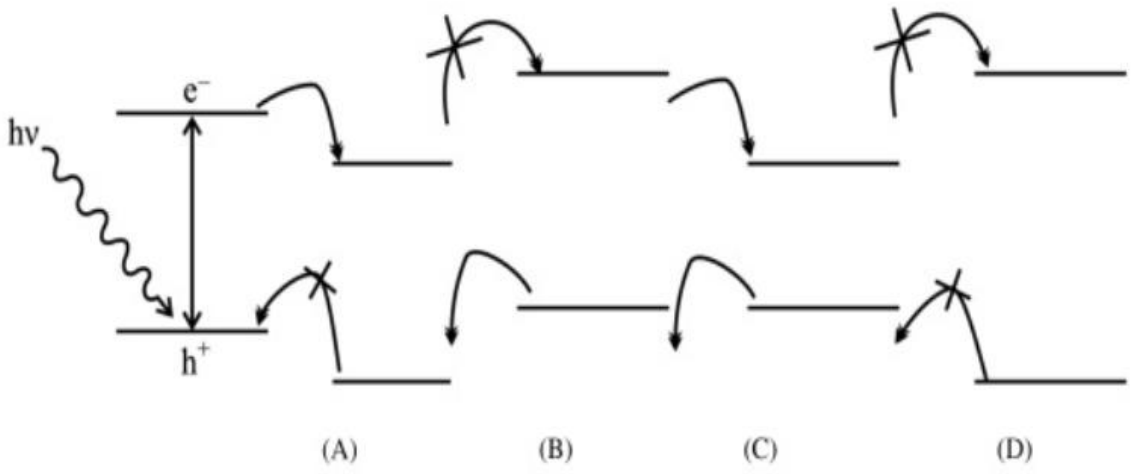

Figure 2.1: Different possibilities of reactions. (A) Reduction. (B) Oxidation. (C) Redox reaction. (D) No reaction (Ameta et al., 2018)

(A) Reduction of substrate takes place, when the redox level of substrate is lower than the conduction band of the semiconductor.

(B) Oxidation of substrate takes place, when the redox level of the substrate is higher than the valence band of the semiconductor.

(C) Neither oxidation nor reduction is possible, when the redox level of the substrate is higher than the conduction band and lower than the valence band of the semiconductor.

(D) Both reduction and oxidation of the substrate take place, when the redox level of the substrate is lower than the conduction band and higher than the valence band.

2.2 Titanium(IV) Oxide (TiO_2)

TiO_2 has drawn the attention of many nanomaterial researchers due to its high potential for energy sector, as well as for environmental protection application which is the focus of this project. Besides, due to its other attractive qualities such as good optical properties, low cost, high photocatalytic activity, chemical stability and non-toxicity, TiO_2 is also being used in many other areas such as disinfectants and antibacterial agents, self-cleaning surfaces, food and pharmaceutical additives, pigments, sensors and many more (Dontsova et al., 2020).

According to a review done by Coronado et al. (2013), since decades ago TiO_2 has captured the attention of many researchers due to its capacity to be photoactivated by solar light, which has then opened up many applications for it such as in heterogeneous photocatalysis, self-cleaning coatings and electrical energy production. Based on a survey in the ISI Web of Knowledge in the period of 2008 to 2012, Coronado et al. (2013) stated that roughly 67% of the articles about photocatalysis are based on the use of TiO_2, showcasing the prominent position of TiO_2 as photoactive material. One of the advantages of TiO_2 over other semiconductors as a photocatalyst is that it allows simultaneous oxidation of hydrogen and reduction of oxygen due to its electronic structure, where the bottom of its conduction band (CB) is more negative than the reduction potential of H^+/H_2 (E_{NHE} = 0.00V), and the top of its valence band (VB) is more positive than the oxidation potential of O_2/H_2O (E_{NHE} = 1.23V) (Chen & Mao, 2007).

Thus, TiO_2 have balanced electrochemical properties unlike other semiconductors such as silicon, which is more efficient for water reduction and SnO_2, which is more efficient for water oxidation (Coronado et al., 2013). On top of that, Coronado et al. mentioned that the surface OH- groups can act as donor species that will react with the

holes from TiO_2 VB to produce hydroxyl radicals, •OH which has very high oxidation potential of $E_{NHE}(•OH/H_2O)$ = 2.27V hence an important intermediate in photocatalysis. Furthermore, they added that TiO_2 can preserve its structural integrity after photocatalytic activity as they do not suffer from anionic photocorrosion. This is because the oxidation of water to form H^+ ions and O_2 molecules is thermodynamically more favored than the formation of O_2 molecules from oxide anions, hence TiO_2 possesses high stability even at extreme pH values in aqueous solution.

Apart from some high-pressure TiO_2 phases, there are three important TiO_2 polymorphs that can be prepared without using special synthesis conditions. These are anatase, rutile and brookite. All these phases, according to Coronado et al. (2013), are arrangement of slightly deformed TiO_6 octahedra connected by vertices or edges, while oxygen shows a threefold coordination. Figure 2.2 below shows the crystal structure of the three phases and Table 2.1 is a short summary of the difference between the three phases.

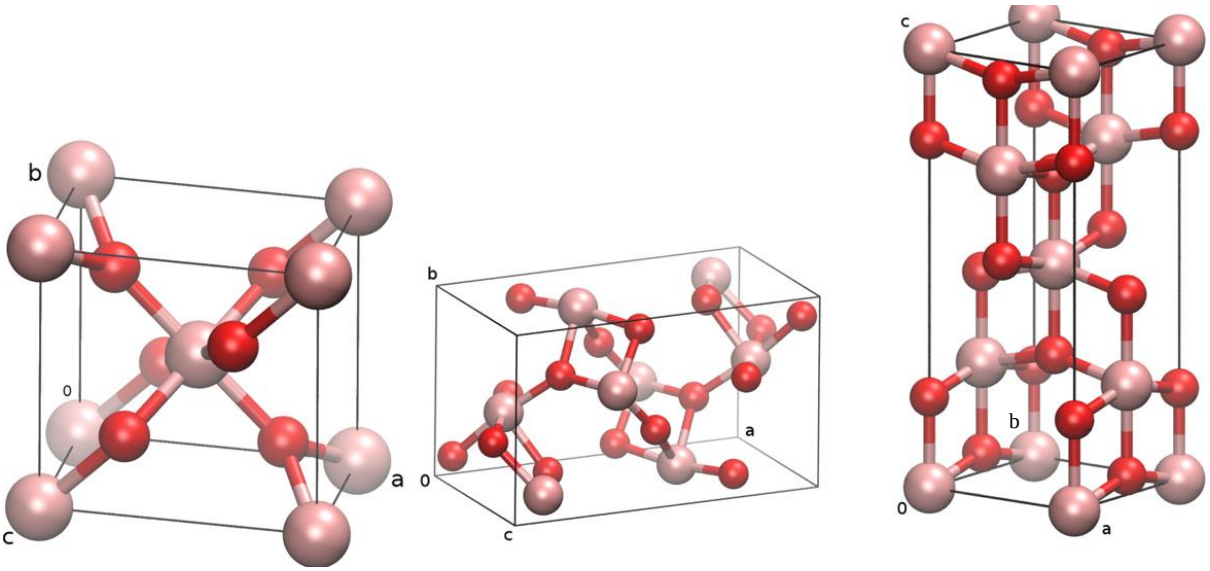

Figure 2.2 Crystal structures of rutile, brookite and anatase (left to right) (Moellmann et al., 2012)

Table 2.1: Crystal properties of rutile, brookite and anatase (Oi et al., 2016)

	Rutile	Brookite	Anatase
Crystal structure	Tetragonal	Orthorhombic	Tetragonal
Atoms per unit cell (Z)	2	8	4
Crystal size (nm)	>35	11-35	<11
Lattice parameters (nm)	a = b = 0.4594, c = 0.2959	b = c = 0.5436, a = 0.9166	a = b = 0.3785, c = 0.9514
Density (g cm^{-3})	4.24	4.17	3.83

Rutile phase is thermodynamically the most stable TiO_2 polymorph at all temperatures and pressures below 60 kPa, but the Gibbs free energy differences between rutile, brookite and anatase are small (around 4 to 20 kJ mol^{-1}), so brookite and anatase can be obtained as metastable phases (Zhang & Banfield, 2000; Chen & Mao, 2007). At low temperature, the transformation of anatase to rutile occurs at an insignificant rate; however, at 600°C, the transformation takes place in pure TiO_2 by surface nucleation and growth mechanism (Carp et al., 2004). Therefore, Coronado et al. (2013) stated in their review on TiO_2 that after low-temperature treatments, anatase or anatase-brookite mixtures will be obtained, although poorly crystallized or amorphous TiO_2 may constitute a large proportion

of it. Rutile phase on the other hand usually starts to appear following calcination at moderate temperatures (300-500°C and becomes the predominant phase after high temperature treatments (>600°C) (Coronado et al., 2013).

The bandgap for rutile, anatase and brookite phases are 3.0eV, 3.2eV and 3.45eV respectively. In terms of photocatalytic abilities of TiO_2 phases, different research suggests different outcome, but after reviewing multiple articles, Coronado et al. (2013) concluded that generally anatase is considered as the most photoactive TiO_2 phase. Factors that may contribute to this difference include variations in electronic, surface structure, and crystalline size. In terms of crystalline size, rutile tends to be larger than anatase due to thermodynamic constrains and thus it has lower surface area and poorer photocatalytic activity than anatase. However, for some pollutants like dye orange 7, pure rutile is more active than anatase (Ryu & Choi, 2008), whereas for others like phenol and trichloroethylene, anatase showed better activity than rutile as shown in Figure 2.3 (Hernández-Alonso et al., 2009).

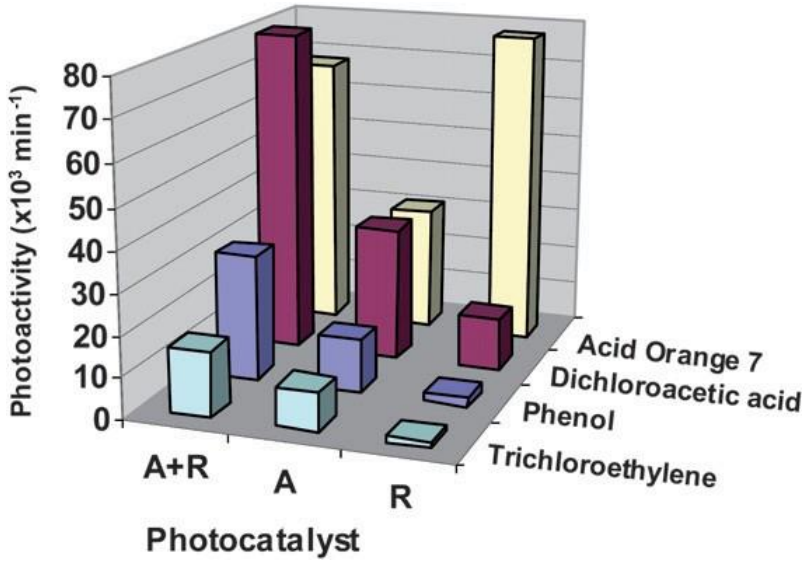

Figure 2.3: Initial rate for the decomposition of four different pollutants in aqueous solution using different TiO_2 commercial photocatalysts with anatase structure (A,

Millenium), rutile (R), or a mixture of rutile and anatase (A+R, Evonik-Degussa P25) (Hernández-Alonso et al., 2009)

From the figure, it can also be seen that biphasic TiO_2 showed better photoactivity than single phase TiO_2, particularly in aqueous solutions. The mentioned anatase-rutile mixture, which is Evonik-Degussa P25, is a commercially available TiO_2 powder with anatase and rutile nanocrystallites in ratio of approximately 15:80, together with less than 5% of amorphous phase. A common justification to the superior performance of biphasic TiO_2 is the formation of heterojunction between the two TiO_2 phases. The bandgap difference between anatase and rutile facilitates charge separation and reduce the electron-hole recombination rate (Coronado et al., 2013). This theory is in good agreement with the findings by Wu et al. (2004), where the photoactivity was found to improve when the degree of interaction between anatase and rutile powdered mixtures increases.

Some works also reported that brookite can have better photoactivity than other TiO_2 phases, although the results can be significantly influenced by the morphological characteristics of the samples involved (Li & Gray, 2007). Lastly, the degree of crystallinity also affects the photoactivity of TiO_2 because structural defects can act as recombination centers (Coronado et al., 2013). In fact, Henderson (2011) reported that amorphous TiO_2 has significantly lower photoactivity than crystalline TiO_2.

2.2.1 Limitation of TiO_2

The photocatalytic performance of pure TiO_2 is rather limited compared to other semiconductors. Taking silicon as an example, the photon-to-current efficiency (IPCE) is about 100% under illumination at 600nm, however for TiO_2 the IPCE is only around 45%

at illumination at 400nm (Hernández-Alonso et al., 2009; Chen & Mao, 2007). Another drawback of TiO_2 as photocatalyst is its wide bandgap, meaning that pure TiO_2 can only absorb light with wavelength in the UV range or shorter. Due to their wide band gap, TiO_2 can only absorb less than 5% of solar energy, making the development of solar technologies that are based on TiO_2 a challenge (Ohtani, 2010). Rapid recombination of these electron-hole pairs is another challenge for TiO_2 photocatalyst (Hosseini-Savari et al., 2018).

2.3 Semiconductor Heterojunction

Various photocatalysts that are based on semiconductor materials have been studied. However, according to Xu et al. (2018), these photocatalysts have limited efficiency for practical applications due to the photogenerated electron-hole pairs recombining too easily as the result of strong attraction force between negatively charged electrons and positively charged holes. On top of that, they also added that for single-component photocatalysts, achieving strong redox ability always comes at the cost of narrowing the light response range of the photocatalyst, and vice versa. They explained that this is because a strong redox ability requires a large band gap, whereas a good light harvesting capability requires a small band gap. To overcome this challenge, design of heterojunction structures is being developed. This section will discuss about the possible charge transfer mechanisms in a semiconductor heterojunction.

A constructed heterojunction is assembled by two semiconductors with staggered band structure configuration, and with this it is now possible to ensure good separation between photogenerated electron-hole pairs, at the same time combining the respective advantages of each semiconductor component (Xu et al., 2018). There are three types of

heterojunction: Type I (straddling gap), II (staggered gap) and III (broken gap) (Zhang et al., 2012) as shown in Figure 2.4, each with different relative positions of CB and VB.

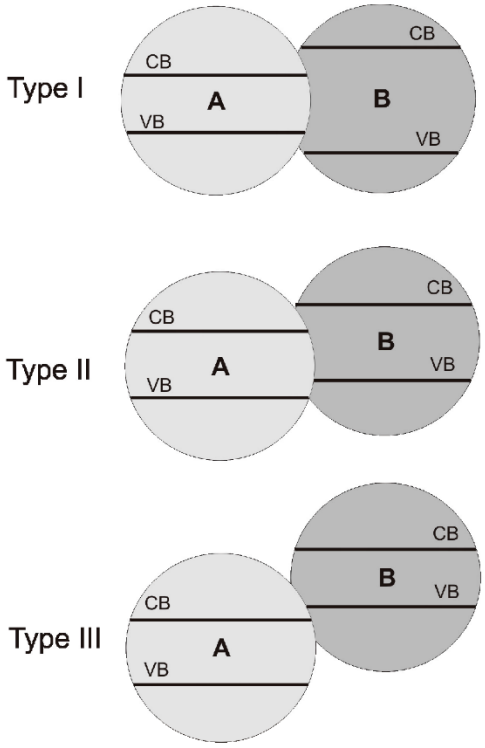

Figure 2.4: Types of heterojunction system of coupled semiconductors (Janczarek & Kowalska, 2017)

Among the three heterojunction types, Janczarek and Kowalska (2017) pointed out that type II has the optimum relative positions of energy bands for efficient charge carrier separation. They explained that the photogenerated electrons are transferred directly from CB(PC I) to CB(PC II) (as in Figure 2.5) due to favorable energetics from the relative positions of CB, or due to band bending at the interface inducing and internal electric field. At the same time, the photogenerated holes are transferred from VB(PC II) to VB(PC I). The accumulated electrons in CB(PC II) are responsible for reduction reactions whereas the accumulated holes in VB(PC I) are responsible for oxidation reactions. Now that the

photogenerated electrons and holes are accumulated in different component, the recombination probability of the electron-hole pairs is reduced due to spatial separation and hence the lifetime of charge carriers is increased (Janczarek & Kowalska, 2017). However, this advantage comes at the cost of reduced redox abilities of charge carriers, meaning that the driving force for photocatalytic reaction is weak which may result in the reaction not occurring (Xu et al., 2018). In fact, its redox ability is less than the redox ability of each individual component of the heterostructure, which means only photochemical processes with ΔG smaller than each semiconductor component of heterostructure can occur, despite having better charge carrier separation and wider spectral range of light absorption (Murashkina et al., 2019).

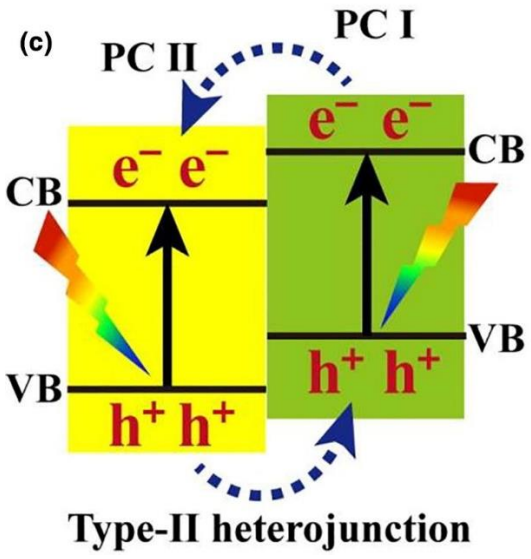

Figure 2.5: The charge transfer in a type II heterostructure (Xu et al., 2018)

2.3.1 Z-Scheme Photocatalytic Systems

To overcome the weakness of type II heterojunction, the charge transfer mode of photogenerated electron-hole pairs is manipulated into direct Z-scheme mode as shown in Figure 2.6 below, which is a more desirable form of constructed heterostructure.

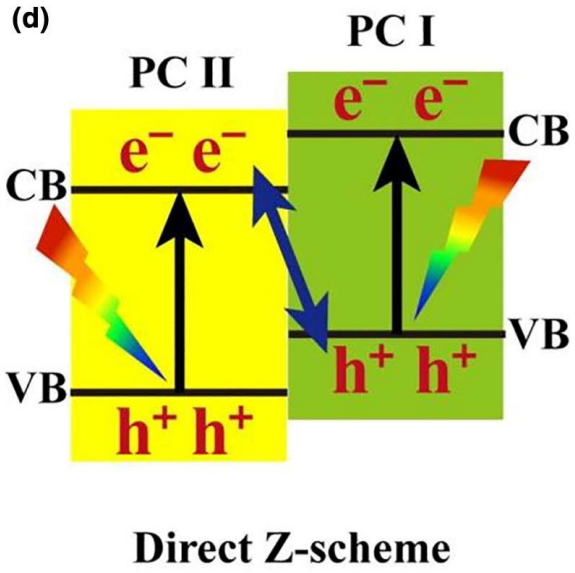

Figure 2.6: The charge transfer in a direct Z-scheme heterostructure (Xu et al., 2018)

Z-scheme photocatalyst can be classified into three distinct types: (1) traditional Z-scheme photocatalysts, (2) all-solid-state Z-scheme photocatalysts and (3) direct Z-scheme photocatalysts. In a traditional Z-scheme photocatalyst, a reversable redox ion pair such as Fe^{3+}/Fe^{2+} or IO^{3-}/I^{-} is employed to serve as the medium for charge carrier transfer. All-solid-state Z-scheme photocatalysts on the other hand are second generation (2006) Z-scheme photocatalysts, where an electron conductor such as Au or Ag nanoparticles are incorporated into the heterostructure to facilitate the transfer of charge carrier. Lastly, direct Z-scheme photocatalysts are third generation (2013) Z-scheme photocatalysts, where a direct contact between two semiconductors is ensured without needing any charge carrier transfer mediator, instead the charge carrier transfer is driven by the internal electric field.

Each of the Z-scheme photocatalysts has different synthetic processes, working mechanisms, properties, and applications (Xu et al., 2018). The topic of this project is on the coupling of two metal oxide semiconductors without the addition of other materials, hence the focus will be mainly on direct Z-scheme and type II heterojunction photocatalytic system (Xu et al., 2018).

2.3.2 Direct Z-Scheme Photocatalysts

When two semiconductors, PC I and PC II (as in Figure 2.7) come into contact, free electrons in PC I are transferred into PC II until their Fermi levels are equilibrated, as shown in Figure 2.7(a). Now, PC I side becomes positively charged while PC II side becomes negatively charged at the interface, forming an internal electric field across the interface and bending the band edge. When photon of sufficient energy hits the photocatalysts, electron-hole pairs are generated in both PC I and PC II. The direction of electric field formed favors the Z-scheme charge transfer mode, meaning that recombination between photogenerated electrons in CB(PC II) and photogenerated holes in VB(PC I) will occur. Besides, other factors such as extra potential barrier induced from band bending and Coulomb repulsion hinder the transfer of photogenerated electrons from CB(PC I) to CB(PC II), as well as photogenerated holes from VB(PC II) to VB(PC I). The recombination of photogenerated electrons from CB(PC I) to VB(PC II) is also hindered due to the presence of induced electric field (Xu et al., 2018).

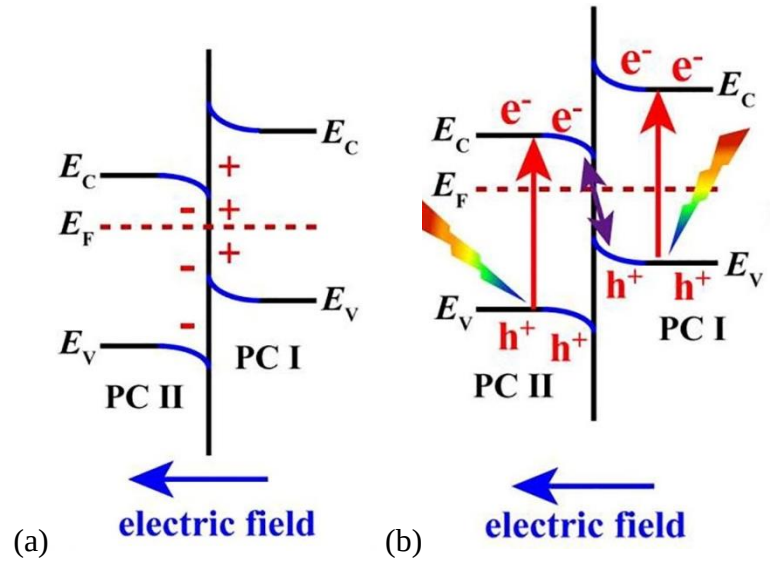

Figure 2.7: Semiconductor-semiconductor junction with staggered band configurations (a) in contact without photon irradiation (b) in contact with photon irradiation (Xu et al., 2018)

The charge transfer mechanism in direct Z-scheme photocatalysts must not be confused with the mechanism in p-n junctions. When a p-type semiconductor meets an n-type semiconductor, free electrons from the n-type semiconductor are transferred to the p-type semiconductor, forming an internal electric field and hence a p-n junction is produced (Figure 2.8(a)). When electron-hole pairs are generated in each semiconductor due to photon excitation, the direction of the internal electric field does not favor the direct Z-scheme charge carrier transfer mode, instead it favors the transfer mechanism as shown in Figure 2.8(b) (Xu et al., 2018).

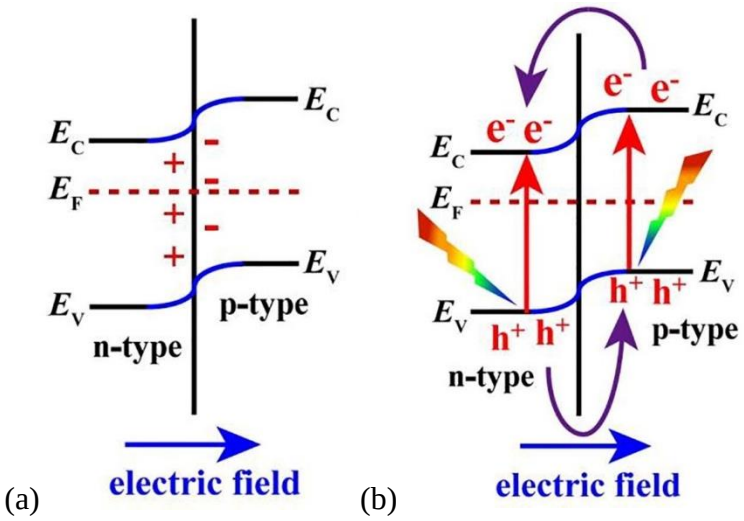

Figure 2.8: p-n junction (a) in contact without photon irradiation (b) in contact with photon irradiation (Xu et al., 2018)

2.4 Modification of TiO_2 through Coupling

To establish heterojunctions for the enhancement of photocatalytic activity, TiO_2 can be coupled with other components like metals or semiconductors. Coupled TiO_2 can be synthesized in various ways such as sol-gel method, hydrothermal method, impregnation method, photodeposition method etc. The 3 metal oxides were selected in this project was based on their bandgap relative to anatase TiO_2 (3.2 eV). CuO has smaller bandgap than TiO_2 (1.6 eV); SnO_2 has larger bandgap than TiO_2 (3.6 eV); ZnO has bandgap that is almost similar with TiO_2 (3.3 eV). The purpose was to study how the relative bandgap affects the outcome photocatalytic properties. Photodeposition and thermal oxidation was used to achieve coupling because it is a relatively cheap and straight-forward method.

2.4.1 CuO/TiO_2 Photocatalyst Composite

CuO is a p-type semiconductor with an optical band gap of 1.6 eV. There are different opinions and findings on the photocatalytic properties by coupling TiO_2 with CuO. Although CuO can absorb more photons due to its relatively small band gap, its CB and VB position makes it less suitable for creating hydroxyl and superoxide radicals which are crucial for the photodegradation of organic pollutants. Song et al. (1999) have found that coupling copper oxides on TiO_2 has reduced its ability to photodegrade 1,4-dichlorobenzene, because the photogenerated electrons cannot move efficiently between the oxides and TiO_2. Besides, Chiang et al. found that CuO has hindered the photodegradation of cyanide by TiO_2 at more than 0.1 atomic percentage of Cu, mainly due to the CuO blocking the surface of TiO_2 as well as increased recombination of photogenerated holes with electrons trapped by the CuO. However, Arana et al. coupled TiO_2 with CuO and found that the photooxidation of tert-butyl ether has improved compared to uncoupled TiO_2. They suggested because Cu^{2+} in the CuO can accept electrons in CB to convert into Cu^{+} to reduce electron-hole pair recombination. The Cu^{+} will then be converted back into Cu^{2+} via reaction with other oxidizing species. CuO/TiO_2 is selected in this project to determine the effect of coupling CuO with TiO_2 on the photodegradation of RhB dye.

2.4.2 ZnO/TiO_2 Photocatalyst Composite

ZnO is also a common option to be coupled with TiO_2. ZnO has almost similar band gap energy with anatase TiO_2 at around 3.3eV (Das et al., 2020). ZnO has hexagonal unit cell instruction called Wurtzite, as well as large exiting binding energy and large bond

strength in room temperature (Mohammadi & Ghorbani, 2018). ZnO shows many promising properties such as high surface reactivity and photosensitivity, economical price, anti-bacterial effect and chemical stability (Mousa et al., 2021), hence attracting researchers to use ZnO for short-wavelength optoelectronic applications as well as water splitting, water detoxification and photoreduction (Mohammadi & Ghorbani, 2018). When irradiated by UV light (<400nm), ZnO nanoparticles can produce hydroxyl radicals, •OH which act as an important oxidizing agent in photodegradation reaction as well as antibacterial activity (Mousa et al., 2021). However, Mousa et al. (2021) also added there are a few limitations of ZnO such as it is susceptible to photo-corrosion effect during photocatalytic process (unlike TiO_2), and its wide bandgap limits UV light absorption at about 5%.

Like other metal oxide semiconductors, ZnO can also be coupled with TiO_2 to enhance the photocatalytic performance. Calgary et al. (1995) have synthesized ceramic-supported TiO_2-ZnO-based films to degrade a textile industry azo dye under UV illumination and has shown improved photocatalytic performance compared to pure biphasic TiO_2 (80% anatase; 20% rutile). Under UV illumination, the generated electrons from the CB of ZnO transfer to CB of TiO_2 while the generated holes transfer from VB of TiO_2 to VB of ZnO, improving the charge separation and charge carrier lifetime (Calgary et al., 1995; Mousa et al., 2021). The electrons accumulated at the TiO_2 can react with oxygen molecules adsorbed on the surface to produce superoxide radical ($•O^{2-}$), then the holes are accumulated at the ZnO surface. Both superoxide radical and holes play an important role in photocatalytic degradation of dyes. Mousa et al. (2021) reported that upon the formation of TiO_2/ZnO heterojunction, the overall bandgap has decreased to around 1.17eV. TiO_2/ZnO heterojunction has higher photocurrent than single oxide materials due to the tight heterojunction between ZnO and TiO_2 (Li et al, 2014).

2.4.3 SnO_2/TiO_2 Photocatalyst Composite

Just like other metal oxides, SnO_2 plays an important role in TiO_2 structures due to the production of more hydroxyl radicals. SnO_2 has larger bandgap (~3.6eV) than both anatase TiO_2 (3.2eV) and rutile TiO_2 (3.0eV), and the CB of SnO_2 is 0.5V more positive than that of TiO_2 (Dontsova et al., 2020). Ti^{4+} and Sn^{4+} have close ionic radii (0.605Å and 0.69Å respectively) and similar structural (tetragonal structure of rutile type) and electronic properties. Nithyadevi and Rajendrakumar (2013) has found that for TiO_2/SnO_2 synthesized with sol-gel method, low and high concentrations of tin precursor give different form of product. At low concentration, a solid solution is obtained whereas at high concentration, TiO_2/SnO_2 nanocomposites are obtained instead. Hou et al. (2007) have synthesized TiO_2 nanowires coupled with different percentage of SnO_2 (0, 2, 5, 10, 15 wt%), and discovered that the photocatalytic performance of the nanocomposite increases up until 5 wt% of SnO_2, and decreases when SnO_2 content is more than 5 wt%. They proposed that the presence of SnO_2 in small amount enhances the photocatalytic property of the nanocomposite by suppressing the charge carrier recombination. The charge carriers in TiO_2/SnO_2 heterojunction follow the double charge transfer mechanism as shown in Figure 2.9 below. From the figure, the photogenerated electrons are accumulated in the CB of SnO_2 which is lower than the CB of TiO_2, whereas the photogenerated holes are accumulated in the VB of TiO_2, which is higher than the VB of SnO_2.

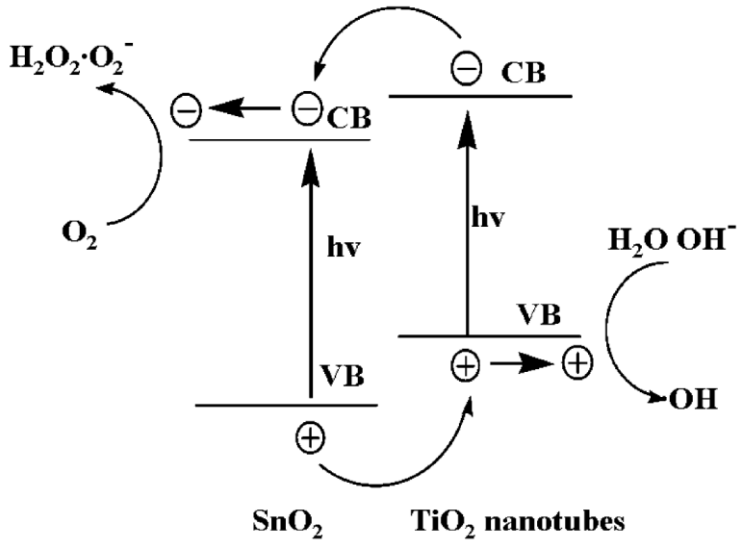

Figure 2.9: Schematic diagram of the charge-transfer process in the TiO_2/SnO_2 nanotubes composite photocatalysts (Hou et al., 2007)

On top of that, Hou et al. (2007) added that since TiO_2 has strong adsorption properties, the concentration of target pollutant around its surface is high, as well as the collision rate between the pollutants and photocatalyst, so the photocatalytic activity is better than pure TiO_2 and SnO_2. However, at higher percentage of SnO_2, less TiO_2 surface is exposed and hence its adsorption property decreases, lowering the photocatalytic activity. On top of that, when SnO_2 is beyond monolayer coverage, the distance of TiO_2 from surface of the photocatalyst will increase, so hole and electron cannot be separated effectively.

2.5 Structure and Morphologies of Photocatalysts

As mentioned in the previous sections, coupling a material (core) with a different material (shell) can alter its properties, like in the case of coupled photocatalysts. The coupling material (the shell) can be in various morphologies, such as particulate, porous and uniform shell which are the focused morphologies of this project. According to a review by Mondal & Sharma (2016), depending on their applications, the properties of

core-shell structured materials may be modified by changing the size and shape, such as changing the size of the core material, the thickness of the shell material, or the porosity of core and shell material. Each core-shell nanostructure has their distinct characteristics. Such composite materials have been used in a wide variety of fields, ranging from biomedical like drug delivery and cancer treatment, to electronics like field effect transistors and sensors. Some research even went as far as adding various chemical functional groups or attaching other molecules onto ordinary core-shell nanoparticles with thin film shell to achieve better material properties. Mondal & Sharma (2016) have given many examples of possible core-shell nanostructures as shown in Figure 2.10 below. The core and the shell can be made up of various materials, such as semiconductors, metals, alloys, polymers, graphene, carbon nanotubes, quantum dots and many more. The core and the shell can even be the same material but with different structures.

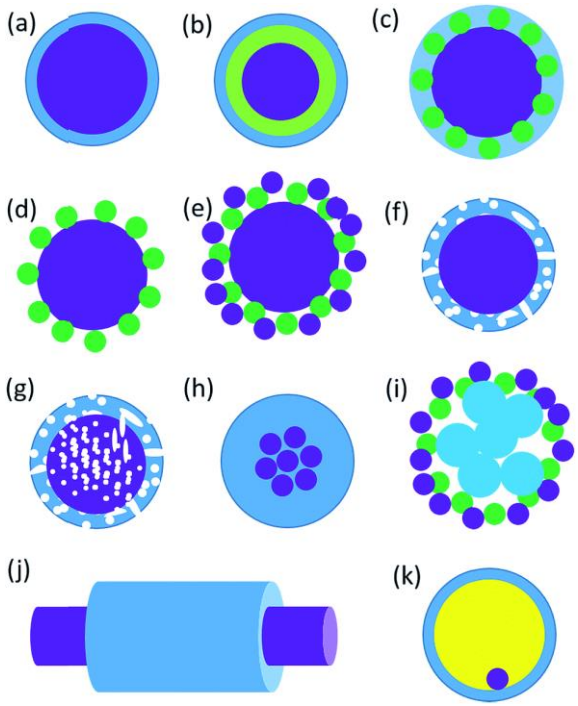

Figure 2.10: Different core–shell nanostructures: (a) core is a single sphere, (b) core with multiple concentric shells, (c) shell incorporated with smaller spheres, (d) shell in the form of identical smaller spheres, and (e) shell in the form of different spheres, (f) solid core and porous shell, (g) core–shell both porous, (h) multiple spherical cores, (i) multiple cores covered by shell formed by several small spheres, (j) core–shell fiber, and (k) yolk–shell morphology shows a movable core within a hollow shell. (Mondal & Sharma, 2016)

In this project, assuming that TiO_2 can be treated as a spherical core, with photodeposition of metal on the TiO_2 core followed by thermal oxidation, three morphologies can potentially be created: (i) discrete metal oxide particulates on the surface of TiO_2 core; (ii) porous, continuous layer of metal oxide on TiO_2 core; and (iii) non-porous, continuous layer of metal oxide on TiO_2 core. The morphologies (i), (ii) and (iii) mentioned resembles the morphologies (d), (f) and (a) respectively in Figure 2.10.

Photocatalytic activity of a photocatalyst is closely related to the time taken for the photogenerated electrons and holes to get into in with the reactant species, thus making the